



HAL
open science

Sanding and analysis of dust from nano-silica filled composite resins for stereolithography

Christophe Bressot, Martin Morgeneyer, Olivier Aguerre-Chariol, Jacques Bouillard, Kevin Zaras, Germ W. Wisser, Robert J. Meier

► **To cite this version:**

Christophe Bressot, Martin Morgeneyer, Olivier Aguerre-Chariol, Jacques Bouillard, Kevin Zaras, et al.. Sanding and analysis of dust from nano-silica filled composite resins for stereolithography. Chemical Engineering Research and Design, 2020, 156, pp.23-30. 10.1016/j.cherd.2020.01.011 . ineris-03318307

HAL Id: ineris-03318307

<https://ineris.hal.science/ineris-03318307>

Submitted on 9 Aug 2021

HAL is a multi-disciplinary open access archive for the deposit and dissemination of scientific research documents, whether they are published or not. The documents may come from teaching and research institutions in France or abroad, or from public or private research centers.

L'archive ouverte pluridisciplinaire **HAL**, est destinée au dépôt et à la diffusion de documents scientifiques de niveau recherche, publiés ou non, émanant des établissements d'enseignement et de recherche français ou étrangers, des laboratoires publics ou privés.

Original Article

Sanding and analysis of dust from nano-silica filled composite resins for stereolithography

C. Bressot^{1,*}, M. Morgeneuyer⁴, O. Aguerre-Chariol¹, J. Bouillard¹, Kevin Zaras², Germ W. Visser³, and Robert J. Meier³

¹ Direction de Risques Chroniques, Institut National de l'Environnement Industriel et des Risques (INERIS), Verneuil en Halatte, France

² DSM Additive Manufacturing, 1122 Saint Charles Street, Elgin, IL 60120, USA

³ DSM P.O. Box 1066, 6160 BB Geleen, The Netherlands

⁴ Université de Technologie de Compiègne, Sorbonne Universités, Compiègne, France

Abstract

The aim of this work was to assess whether with high amounts of nano-silica filled cured resins release nano-particles upon their abrasion, as this could form an occupational health risk and require specific safety measures.

A standardised abrasion stress method involving a Taber linear abrasion apparatus (Model 5750) has been applied to the filled polymer samples. This linear abrasion apparatus simulates the mechanical solicitation, i.e. abrasion. Various particle size measurement techniques were applied to assess the size distribution and the quantity of particles released.

Observations of airborne particle from abrasion tests are consistent with TEM characterization of the nanomaterials before any tests. Abrasions of both samples (called here '1' and '2') gave rise to emissions. For sample 1, a few larger 'dust' particles (collected in a bottle) and micronic particles are observed. For sample 2, despite a track on the sample, no detectable micronic particles and very few larger, 'dust', particles are detected. As a result, we can state there were effective abrasions which gave rise to a low emission (sample 1) and a very low emission (sample 2) under the detection limits of particle sizing and counting, for the last case.

The emission of particles upon Taber test abrasion is extremely low (less than 8 particles per cm³) and for one of the samples at the level of the detection limit. Moreover, the size of these particles is generally larger than nano-scale.

Keywords: nano-materials, nanosafety, silica, particle size, occupational health, safe by design

Introduction

The present study investigates the tendency of a 3D printed product **to emit particles** during an important part of its life cycle, i.e. the phase of its use. Many researches have yet been performed on the 3D processes' tendencies to emit particle during the production phase. However, 3D printed products will be more and more present in every day's life and a preliminary study of the potential exposure of workers and consumers to risks related to 3D printed objects is urgently needed.

The study presented here was performed within the context of the NanoREG 2 project, funded by the European Commission under EU's Horizon 2020 Program Research and Innovation actions H2020-NMP-2014-2015. This project includes industrialists from various backgrounds, public institutions and other bodies. The main industrial actor with respect to the research presented here is DSM¹. The primary objective of this project is to develop and implement Safe by Design (SbD) principle for nanomaterials. The present study is devoted to industrial case studies. One of these is the sample 1 involving the handling of silica, blending this with uncured resin, and subsequently photo-curing. This process is executed under safe conditions.

Stereolithography is a 3D-Printing process where a liquid photopolymer resin is cured from a liquid to solid upon exposure to UV light (Jacobs, 1992). This process exposes a thin layer of resin, which then a "slice" of a 3D model is imaged on the thin resin surface to form a solid layer. Subsequent layers are then "printed" upon the previous layer building up a 3-dimensional solid part. This is a common, industrial 3D printing process that has been used for over 20 years for prototyping, modeling and now manufacturing more customized final parts. Compared to other rapid prototyping processes, stereolithography has the advantage of using a liquid-based polymer, since powders are prone to dust release (Kahrizsangi et al., 2015; Salehi et al., 2017).

Some of the materials used in the process are composites, comprised of UV-curable acrylate and epoxy monomers, as well as certain levels of solid particles. Some of the more popular composite resins used in the process contain combinations of nano-silica and fumed or crystalline silica. The addition of particles in the nanorange is being used to improve mechanical properties whilst still keeping a low viscosity resin. The silica content is typically in the order of 50% weight.

Presence of crystalline SiO₂ could be the main observation to take into account due to the regulation on this component(UE, 2017). Thus, the limit values for occupational exposure of respirable crystalline silica dust is established at 0.1 mg/m³. Each Member States of UE shall bring into force the laws, regulations and administrative provisions necessary to comply with this Directive by 17 January 2020.

Within its own internal processes including production and handling processes, DSM has adopted and adheres to the principles of the Program of Responsible Care, set out by the International Council of Chemical Associations ((ICCA), 2019). This encompasses commitment to understand, manage and communicate the use of hazardous substances, in order to develop and sell products that do not pose an unacceptable risk to human, animal and the environment, when applied in the appropriate manner. For the present case this means that all process steps are handled safe as from the beginning (Safe by Design), as illustrated in the figure 1 below. The coating material is solvent free.

¹ Koninklijke DSM N.V. (Royal DSM, commonly known as DSM), is a Dutch multinational active in the fields of health, nutrition and materials.

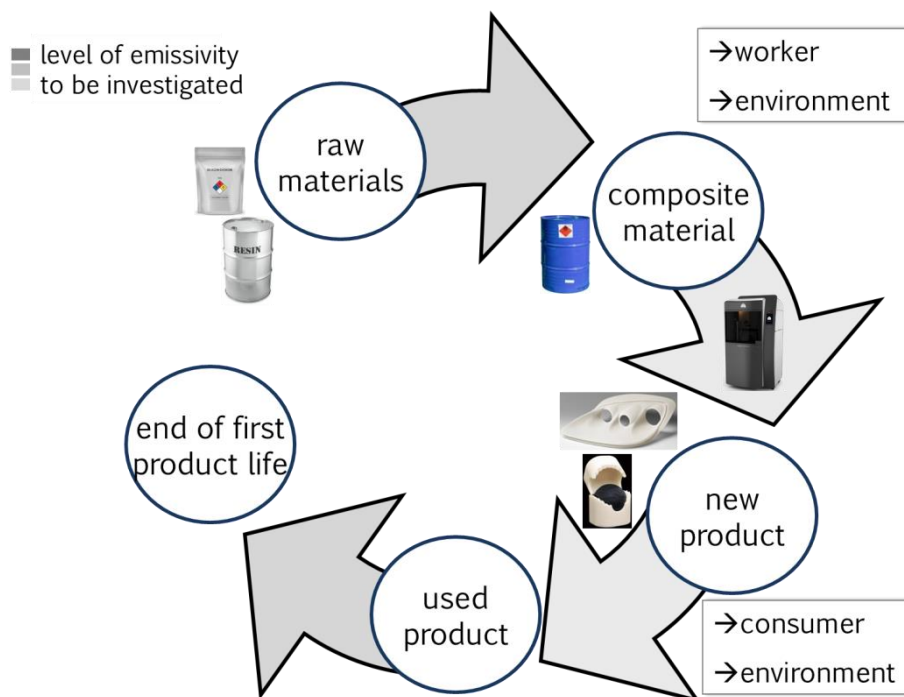


Figure 1. The Safe by Design approach covering parts of the life cycle

Thus, handling of silica, blending with uncured resin, and subsequently photo-curing is executed under safe, i.e. confined conditions.

Nanoparticle exposure at workplaces is a clear concern for policy makers in the EU (Commission, 2014, 2014; Krug, 2014; Seal and Karn, 2014; Arts et al., 2015; ISO, 2017; National Institute for Public Health and the Environment, 2017). That situation gives rise to a large number of solutions to manage the nano-risk (ANSES, 2014; Karim et al., 2015; Liguori et al., 2016). Regarding the impact of nanoparticles on living being (Bouguerra et al., 2019) and their dispersion of nanosized objects on a large scale (Sofia et al., 2018), a 'Safe by Design' approach (SbD) aims at reducing potential health and environmental risks at an early phase of the innovation process, by eliminating or minimising the risk of adverse health effects during its life cycle. To do so, in general, the following SbD guidelines should be followed:

1. Identify and reduce any uncertainties about health risks, products and processes
2. Manage health risks of innovative nanomaterials

The SbD concept can both be used to existing nanomaterials, as well as to innovations that can entail cost/benefit evaluations at the innovation, manufacturing and use stages.

The nano-risk assessment is the evaluation of both the exposure and the hazard of nanomaterial. Inhalation is considered as being the main exposure toxicological route (Daigle et al., 2003). Exposure at workplaces could be assessed by coupling a particle counter and a TEM sampler, making possible a characterization in terms of their number concentration, size, shape and chemical composition (Bressot, Shandilya, et al., 2018). A global comparison of different emission sources at workplace identifies mechanical solicitations on the nanomaterial as one of the most emissive step (Ding et al., 2017). Despite of metrological challenges related to particle characterization (Morgeneyer, Ramirez, et al., 2018), many studies have highlighted the production of nanoparticle emissions under abrasion conditions on coatings (Shandilya et al., 2014), paints (Morgeneyer, Aguerre-Chariol, et al., 2018), tiles (Bressot, Aubry, Pagnoux,

Aguerre-Chariol, et al., 2018). As shown above, sanding solicitation gives rise of debris aerosol on Sample 1 and 2, and a way to reduce emission and human/environmental exposure consists in either containing emissions via special extraction equipment or using matrices with stronger affinities with nanoparticles.

A common practice in the 3D printing industry is to sand the surface of the built part to remove defects and smooth the surface for finishing before applying paint or lacquer. In this sanding process, dust comprised of the composite resin is created and could pose a potential inhalation hazard for the workers sanding the parts and others within the same work area. This study was commissioned to determine if any of the crystalline or nano-particle silica is released during the sanding process that could pose a health risk to workers.

In the recent past several studies on machined nanocomposite materials have been published including (Cena and Peters, 2011), (Golanski et al., 2011), (Koponen et al., 2011), (Schlagenhauf et al., 2012), (Wohlleben et al., 2011), (Huang et al., 2012), (Golanski et al., 2012), (Göhler et al., 2013), (Hirth et al., 2013) and (Gomez et al., 2014), Some of them use the Taber standardized method to study abrasion resistance of materials and coatings abrasion test (Vorbau et al., 2009), (Golanski et al., 2011), (Golanski et al., 2012), (Schlagenhauf et al., 2012), in another a hand-held sanding machine was used (Gomez et al., 2014). In most of the studies no free nanoparticles were observed, whereas the study by (Schlagenhauf et al., 2012) revealed free CNTs were released into the environment from polymers containing CNTs. (Bello et al., 2010) investigated exposures during solid core drilling of CNT-epoxy composites reporting release of CNTs clusters during drilling.

Material and method of abrasion tests

The present study deals with sandpapering two photo-cured products, one containing amorphous nano-silica (the DSM product SOMOS PerFORM, (DSM, 2019; Prototyping, 2019)) whereas the second one contains crystalline silica. Whereas on the one hand nano-crystalline silica is known to be much more hazardous as such compared to amorphous silica, the behaviour during sandpapering filled photo-cured resin products containing a high volume percentage of silica (typically 50%) might be different.

Both polymer composite samples, referred to as sample 1 and sample 2 respectively, primarily consist of 35-50% silica embedded in an epoxy resin based on 3,4-epoxycyclohexylmethyl-3,4-epoxycyclohexanecarboxylate (see (Systems, 2019) and (Desotech, 2006)). For sample 1 the silica is surface treated with propenoic acid, 2-methyl, 3-(trimethoxysilyl) propyl ester which reacts with the epoxy in the final formulation. The resin is UV-photocured resulting in a hard polymer composite. Sample 2 is made of a commercial polymer containing silica with an unknown silica fraction. *Table 1* summarizes the properties of the two samples investigated within this study, according to different ASTM standards.

Table 1: Properties of the two samples investigated within this study, according to different ASTM standards

ASTM Method	Property	1 st sample	2 nd sample	Unit
D638-10	Tensile Strength	~68	66-68	MPa
D638-10	Tensile Modulus	~10,500	7,600-11,700	MPa
D638-10	Elongation at Break	~1.1	1.4 - 2.4	%
D790-10	Flexural Strength	~120	124-154	MPa
D790-10	Flexural Modulus	~10,000	8,300-9,800	MPa
D256-10	Izod Impact (Notched)	17	13-17	J/m

D2240-05	Hardness (Shore D)	94	92	
DMA, E''	Glass Transition (T _g)	72-81	78-81	°C

TEM images were obtained using a JEOL JEM 1400 Plus at 120 kV, fitted with an energy-dispersive spectroscopy microanalysis system (Oxford Instruments AZTEC). Initial TEM characterization of the two samples has been done on thin (100 nm) slices obtained by ultramicrotomy.

The standardised abrasion stress method applies for example to wall claddings, paints, stains and tiles and is copiously described in numerous previous publications (Shandilya et al., 2015; Bressot et al., 2017; Bressot, Aubry, Pagnoux, Aguerre Chariol, et al., 2018). For the experiments presented here, a Taber linear[®] abrasion apparatus (Model 5750; Taber Inc. USA) has been selected. A linear abrasion apparatus simulates the mechanical solicitation. Its original and commercial form, is used in numerous internationally recognized test standards from ASTM (ASTM International, 1996; ASTM International 2007; ASTM International 2008; Bressot et al., 2017). The specimen is constantly in contact with the abrader (H38 abrader, Taber Inc. USA) under a vertical weight. A motor unit allows for a back-and-forth motion of the abrader on the fixed sample, making possible the horizontal motion of an applied vertical normal force. The normal force (F_N) applied on the specimen is estimated to 4.222 N.

According to Golanski et al. (Golanski et al., 2011) due to its robust and user-friendly design, its original form (Model 5750; Taber Inc. USA) is already being widely used in industries for testing products like paint, coating, metal, paper, textile, etc. The stress being applied through this apparatus approximates the typical one applied in a domestic setting, for example, walking with shoes (Hassan et al.; Vorbau et al., 2009). In **figure 2**, a horizontal bar moves the selected abradant in a to and fro motion over the specimen surface. The specimen wear occurs at the contact surface due to the friction. The magnitude of the abrasion wear can be varied by varying the normal load (F_N) which acts at the top of the abradant. By changing the type of the abradant and normal load value, one may vary the abrasiveness and hence the mechanical stress.

The test optimization consists in modifying the parameters to minimize abradant clogging. In our case, the stress protocol entails linear abrasion of a sample for 10 minutes. An H38 abrasive (TABER[®] corundum (Al_2O_3) grains) then rubs back and forth over a 76.2 mm distance at a speed of 60 cycles per minute at minimum possible load level of 4,2N, generating an aerosol that is detected and characterized by a Transmission Electronic Microscope (TEM) using a Mini particle sampler (MPS) to collect aerosols, an Aerodynamic Particle Sizer (APS), a **Condensation Particle Counter (CPC)** and a Scanning Mobility Particle Sizer (SMPS).

The details of the test conditions are summarized in the Figure 2.

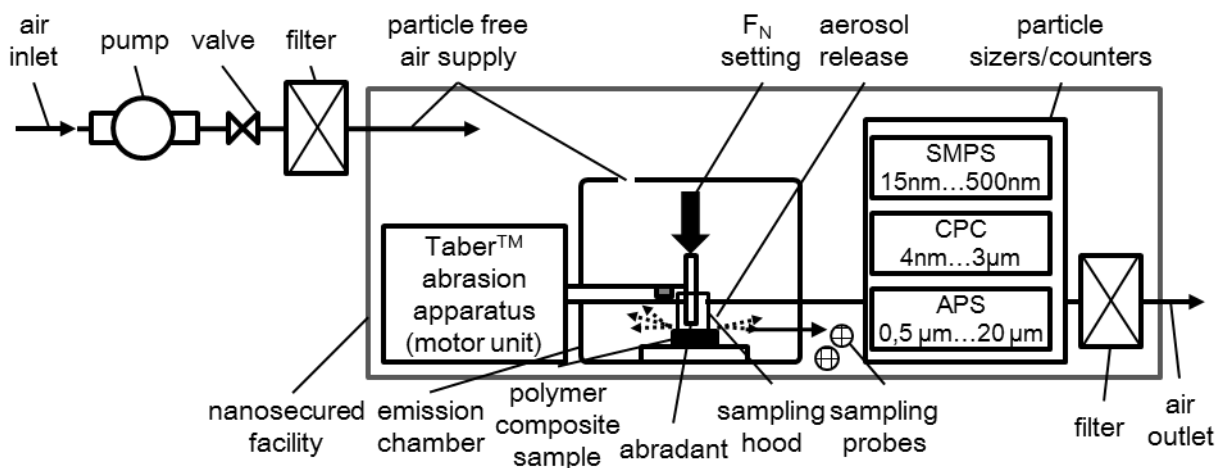


Figure 2 : Schematic overview of the experimental set-up (Bressot et al., 2017).

Each test is preceded by a two-minute measurement to check if the background particle concentration is negligible ($< 1 \text{ \#/cm}^3$). The duration of a TABER abrasion test lasts 10 minutes and is followed by two minutes of purging. The tests are carried out in a sealed chamber in a nanosafe laminar fumehood.

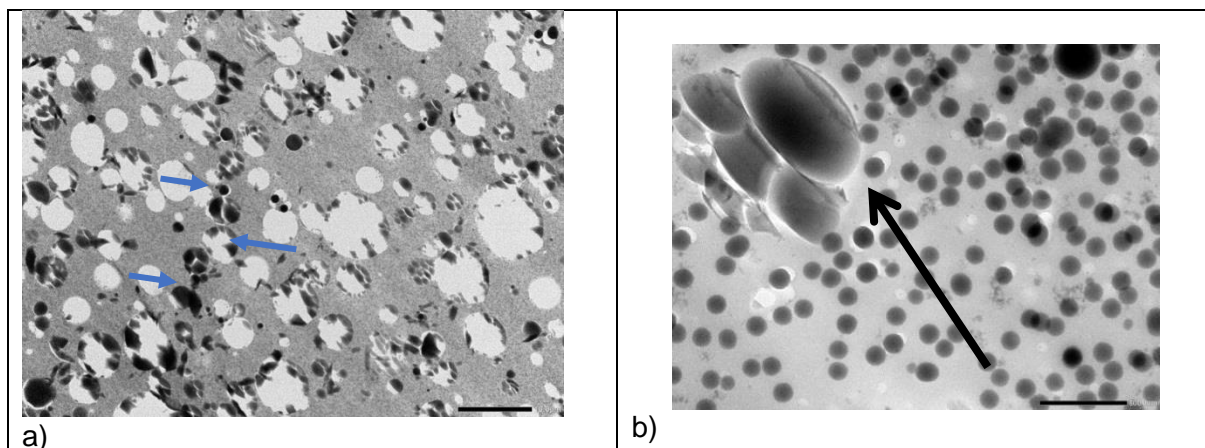
To address more directly the question of the exposure assessment of both studied nanomaterials, these particle releases have been evaluated with respect to their respective solicitation surfaces. To do so, the corresponding surfaces have been estimated.

Results

TEM/EDS analysis on initial bulk specimens (Sample 1 and Sample 2)

The two specimens, sample 1 and sample 2, have been prepared by ultramicrotomy at DSM. Thin (100 nm) slices have then been examined in TEM at INERIS². We observed a good dispersion in both samples (no agglomerates of more than about ten particles, no zones obviously without filler).

Sample 1 revealed a large number of spherical and amorphous particles (*Figure 3 a and b*) with an average size in the range 2-10 micrometers. Most of these particles were removed from the polymer matrix or partially destroyed by the diamond knife during ultramicrotomy, leaving holes in the thin slice (appearing as white circles in *Figure 3 a*).



² FRENCH NATIONAL INSTITUTE FOR INDUSTRIAL ENVIRONMENT AND RISKS

Figure 3 a). TEM image of 100 nm thick slice of sample 1 (scale bar: 10 μm). b) TEM image of 100 nm thick slice of sample 1 (scale bar: 0,5 μm)

At higher magnifications, a great number of smaller (100-150 nm) spherical and amorphous particles were visible Figure 3 b. A few aggregates of smaller individual silica particles were also visible in the polymer matrix (see the blue arrows in Figure 3 a), between the 100-150 nm beads.

Sample 2 revealed a large number of SiO_2 rather large irregular and crystalline particles (see Figure 4 a and b) with an average size in the range 2-10 micrometers. Most of these particles have been removed or partially destroyed by the diamond knife during ultramicrotomy.

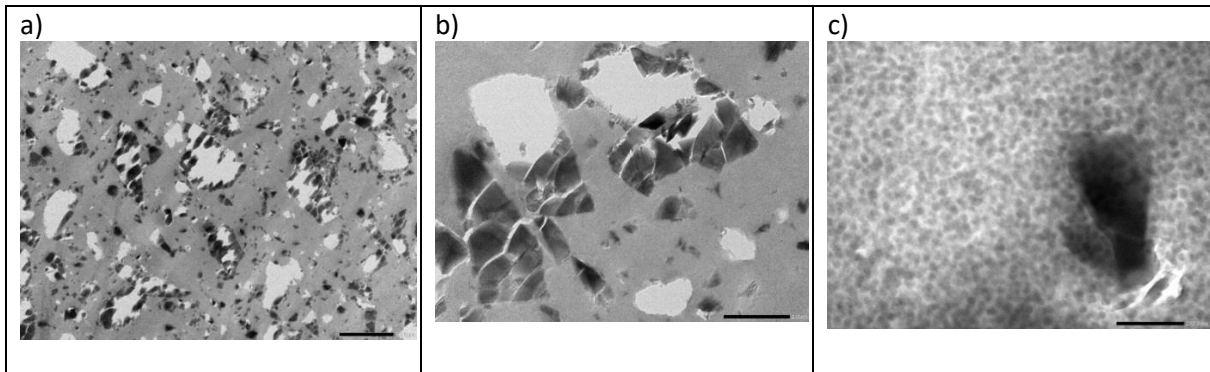


Figure 4 : a) TEM image of 100 nm thick slice of sample 2 (scale bar: 10 μm). b) . TEM image of 100 nm thick slice of sample 2 (scale bar: 2 μm). c) TEM image of 100 nm thick slice of sample 2 (scale bar: 0,2 μm)

At higher magnifications, a great number of very small (20-30 nm) spherical and amorphous particles were visible (Figure 4 c). This very numerous population may have a great effect on mechanical properties, since inter-particle distances were much smaller in sample 2 compared to sample 1. Apart from silica, nothing else is found in the polymer matrix as recognizable particles.

On-line particle counting during abrasion of samples

The CNC (Condensation Nucleus Counter) measurement provided emission number concentrations ($\#/ \text{cm}^3$) between 5 nm and 3 μm . Therefore, it gave a global information about the particulate emissions in the main emission domain (see Figure 5). Sample 1 revealed weak emission under abrasions, distributed between 2 $\#/ \text{cm}^3$ and 8 $\#/ \text{cm}^3$. Sample 2 (see Figure 5) demonstrated a lower emission level below 1 $\#/ \text{cm}^3$ at the same conditions.

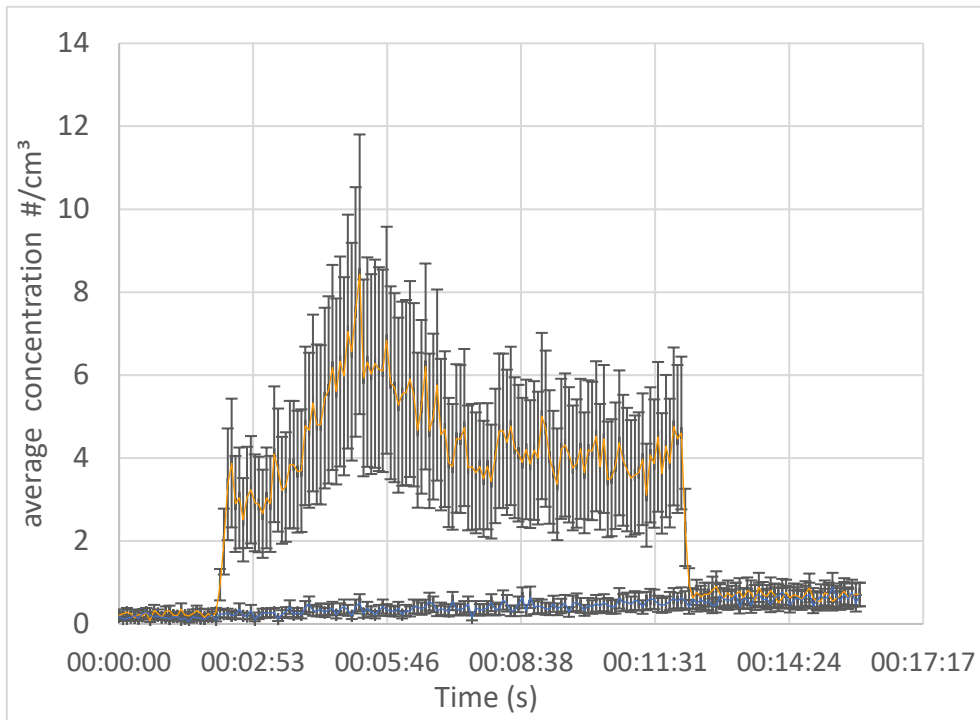


Figure 5 Counting concentrations with standard deviation versus time during abrasion of both sample 1 and sample 2. Average of 3 tests. The abrasion test starts at $t = 2$ minutes and continues 10 minutes. Orange: sample 1; blue: sample 2.

Particle size Distribution measurement with APS ($0.5 \mu\text{m}$ - $20 \mu\text{m}$) during abrasion

In the conditions described above, the emissions of Sample 1 were low, with concentrations below 7 \#/cm^3 . The particle size distribution measured by APS (range between $0.5 \mu\text{m}$ – $20 \mu\text{m}$) of Sample 1 highlights a mode at $2 \mu\text{m}$, with a size distribution spanning between $0.5 \mu\text{m}$ and $8 \mu\text{m}$. A minor fraction was observed below $1 \mu\text{m}$. Sample 2 gave rise to a lower emission (see Figure 6) below the detection limit (1 \#/cm^3). In these conditions, no size characterizations are consequently available for Sample 2.

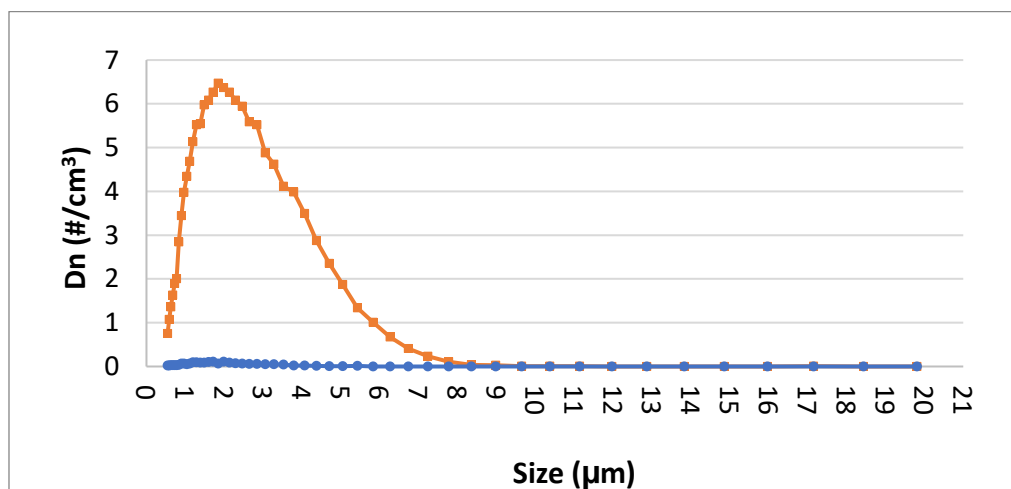


Figure 6 . Particle size distribution measured by APS during abrasion tests on samples 1 and 2. Values are averages on 3 tests of 10 minutes each. Orange: sample 1; blue: sample 2.

Particle size distribution using SMPS

The total counting (range between 15 nm / 673 nm) obtained during the tests were too low to allow a particle size distribution.

Off line measurement: TEM /EDS analysis obtained during abrasions of samples

Sample 1

Due to the low emission level observed during the abrasion, the sampling time duration is extended to 10 min *i.e.* the whole test, instead of 1 min commonly used. In these conditions, many different objects have been observed on the TEM grid. Near polymer matrix debris (see *Figure 7 a* and *b*) quasi spherical particles of 1 micrometre or bigger size were collected (*Figure 7 b*) which are made principally of Si and O. Some smaller objects below 1 μm are detected (*Figure 7 c*). These collected objects consisted of quasi spheres of 120 nm of diameter and were mostly made of Si and O and C (see *Figure 7 c* and *d*). They can be interpreted as silica spheres totally or partially embedded in polymer matrix.

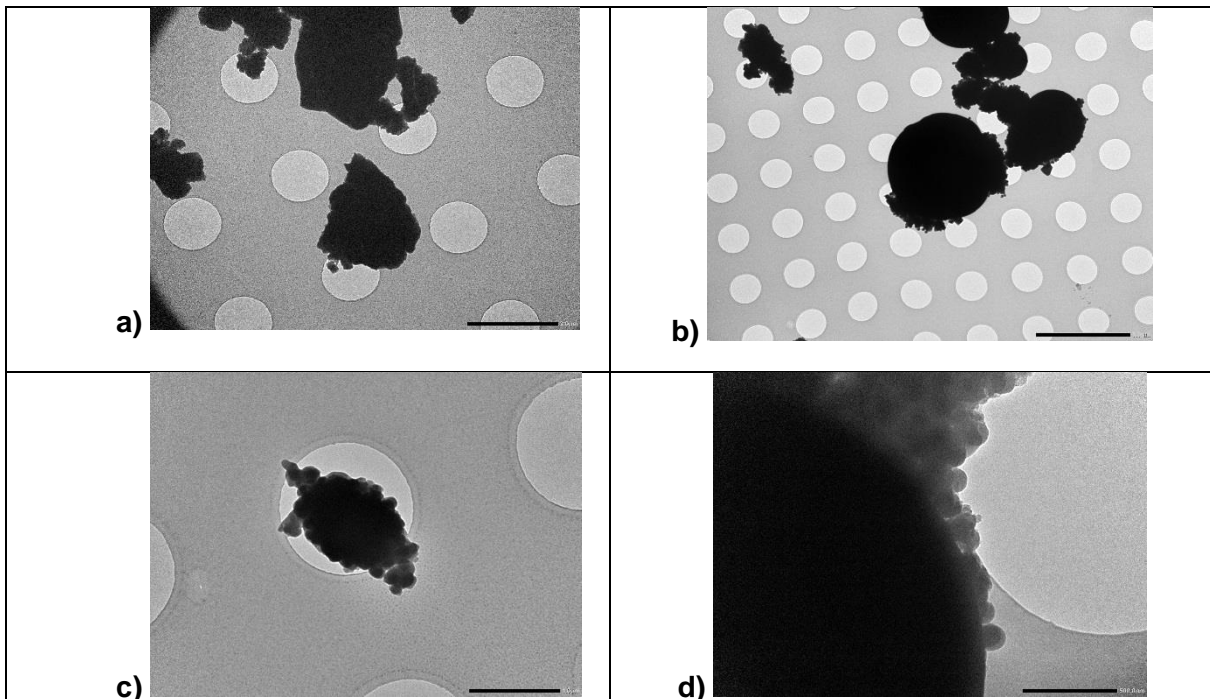


Figure 7: a) overview of the TEM grid with matrix debris. Scale bar 2 μm . b) Quasi spherical particles of 1 micrometer made of Si, O and C (low concentrations). Scale bar 5 μm . c) Smaller particles made of Si, O, and C. Scale bar 1 μm . d) nanosized particles made of SiO_2 on a micronic object. Scale bar 500 nm.

Sample 2

The objects collected during the abrasion of sample 2 were rare (one or two objects per grid square), essentially with two populations, one in the micron size range (see *Figure 8 a*), and one displaying rare submicronic objects (*Figure 8 b*). Micronic objects were big crystalline silica particles with more or less polymer matrix stuck on them (*Figure 8 a*) or polymer debris without big silica particles (*Figure 8 b*). Submicronic objects are polymer debris. At high magnifications, a great number of silica nanoparticles (20-30 nm in diameter) were visible if we look at thin edges (*Figure 8 c* and *d*). The particle sizes of SiO_2 produced with sample 1 and sample 2 are comparable with those observed in the initial materials.

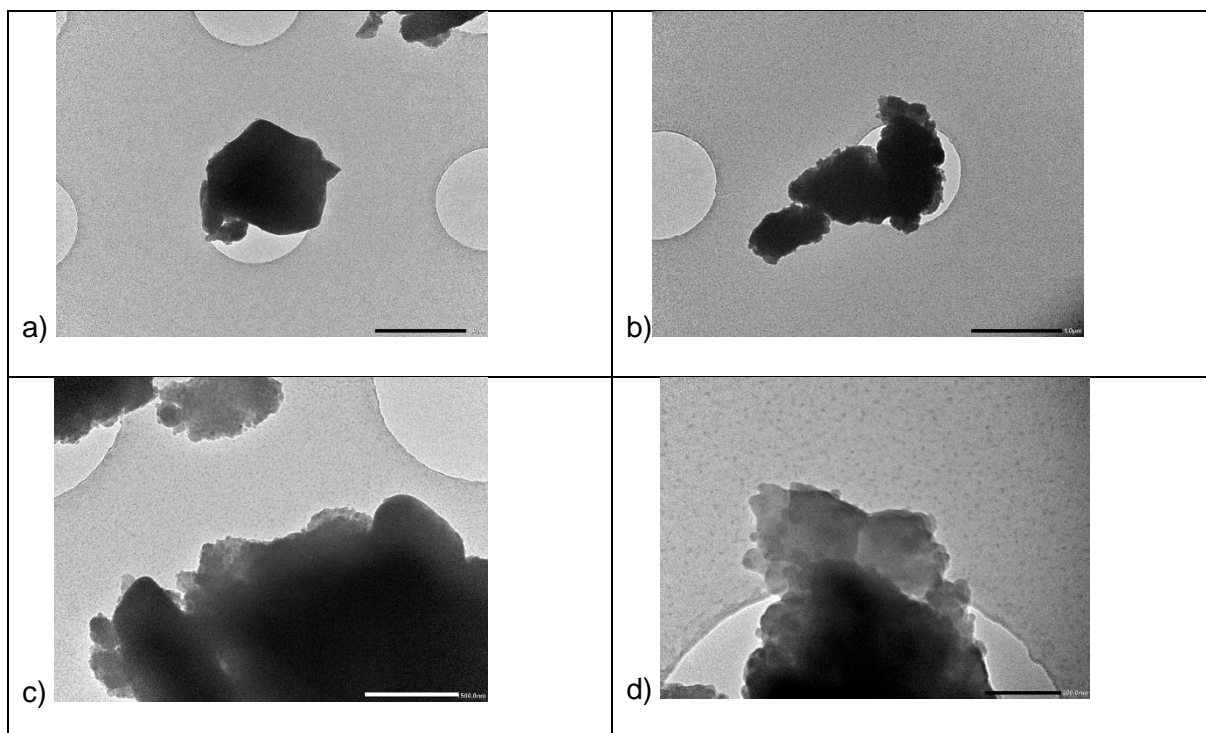


Figure 8: a) Micronic objects collected during the abrasion of sample 2. Scale bar 1 μm . b) Submicronic and micronic objects collected during the abrasion of sample 2. Scale bar 1 μm . c) Submicronic and micronic objects collected during the abrasion of sample 2. Manual sizing and EDS of the nano-objects and agglomerates (NOAA) indicate nanoparticles made of Si and O. Scale bar 500 μm . d) Micronic objects collected during the abrasion of sample 2. Manual sizing and EDS of the NOAA indicate nanoparticles made of Si and O. Scalebar 200 μm .

Discussion

From abrasion tests on both of sample 1 and sample 2, we observe emissions of a few larger 'dust' particles (collected in a bottle) and micronic particles. For sample 2, there are no detectable micronic particles and very few larger, 'dust' particles. As one result we can state that effective abrasions occurred which give rise to a low emission (sample 1) and a very low emission (sample 2), the latter being below the detection limits of sizing and counting.

The emissivity average by surface metrics has been assessed at $6.77 \cdot 10^{-3} \# \cdot \text{cm}^{-3} \cdot \text{mm}^{-2}$ during the abrasion test for Sample 1 and, as already pointed out, under the detection limit for sample 2.

Airborne particle observations from abrasion test are consistent with TEM characterization of the nanomaterials before abrasion tests. If the silica concentrations in both specimens are similar, the type and the size of the silica charges in the nanomaterial seem to influence their emissivity: sample 2 is less emissive, probably since a smaller nano-silica is used, which

increases the contacts between the nanoparticles and the matrix and consequently improve the mechanical reinforcement. It must be noted, however, that the micron particles used (and emitted from) sample 2 are crystalline in nature. Conversely, all silica particles present (and emitted from) sample 1 are amorphous silica.

For the two specimens, a fraction of emitted silica particles and nanoparticles are not completely embedded in the polymer matrix, notably on the edges of the larger objects. The possibility of having direct contact of these nanoparticle with human body may have consequences in terms of toxicity.

Sample 2 contains small SiO₂ (20-30nm), hence with strong bounds to the matrix leading to potential lower emissions, and in this case below the detection limit. Sample 1 contains larger 100-150 nm amorphous SiO₂ less strongly bound, and easier to remove.

In an absolute sense both samples have very limited release and the realised particles are conglomerates of polymer % SiO₂, or mainly micron-sized SiO₂. Emissions from both samples appear to be minimal and mostly micron-sized.

In terms of safe by design, we observe for both specimens very low emissions, however of different natures. Particularly sample 2 releases crystalline silica, which might be problematic in view of the samples use for 3D printing, since this substance is regulated and known for inducing silicosis.

Conclusions

3D printing is now a well-developed technique which is becoming widely spread both in industry as well as in the consumer sector. Emissions during different stages of the lifecycle can be evaluated to assess potential consumer and occupational health risks. Taking into account both prerogatives in terms of public and occupational exposure prevention, this study aimed at providing the methodology to compare material abrasion emission at the level of the source.

The obtained results in lab scale conditions which are presented in this study show very low emission levels for two investigated composites containing nano-silica particles used in 3D printing technologies. Very low exposures (less than 8 particles /cm³) were recorded for both composites, with a lower emission level exhibiting the presence of crystalline nano-silica particles for the composite containing crystalline nano-silica.

A metric defined as particle concentration per abraded surface is proposed to assess the emission at larger abrasion surface scales. This new metric may find useful applications in various exposure scenarios required in risk evaluation.

Acknowledgements

We like to thank Heidi Govaers (DSM) for microtoming the samples and Leo Vleugels (DSM) for useful discussions. Discussions with our colleagues from the EUPLAPSCH network are also gratefully acknowledged. The French Ministry for Ecology funding is gratefully acknowledged.

Funding

The research for this work has received funding from the European Union (EU) project NanoREG 2 (grant agreement n° 646221) under EU's Horizon 2020 Programme Research and Innovation actions H2020-NMP-2014-2015 The views and opinions expressed in this article are only those of the authors, and do not necessarily reflect those of the European Union Research Agency. The European Union is not liable for any use that may be made of the information contained herein.

Contributorship Statement

C.B., M.M. and O.A.-C. performed the abrasion and particle analysis studies, conception and design, acquisition of data and analysis and interpretation of data. K.Z. and G.W.V. have established the case study and provided the materials. R.J.M. guided the case study on behalf of the owner DSM and was involved in writing the draft of the manuscript and the final approval of the version to be published.

References

- (ICCA) TICoCA. (2019) Responsible Care - The Quest for Performance Excellence. Book Responsible Care - The Quest for Performance Excellence, City.
- ANSES. (2014) Evaluation des risques liés aux nanomatériaux, enjeux et mise à jour des connaissances, avril 2014.
- ASTM International. (1996) Standard test methods for dry abrasion mar resistance of high gloss coatings ASTM D6037. .
- ASTM International (2007). Standard test method for the abrasion of organic coatings by the Taber abradant ASTM D4060,
- .
- ASTM International (2008) Standard test method for resistance of transparent plastics to surface abrasion, ASTM D1044.
- Bello D, Wardle BL, Zhang J, Yamamoto N, Santeufemio C, Hallock M, Virji MA. (2010) Characterization of exposures to nanoscale particles and fibers during solid core drilling of hybrid carbon nanotube advanced composites. International journal of occupational and environmental health; 16: 434-50.
- Bouguerra S, Gavina A, da Graça Rasteiro M, Rocha-Santos T, Ksibi M, Pereira R. (2019) Effects of cobalt oxide nanomaterial on plants and soil invertebrates at different levels of biological organization. Journal of Soils and Sediments.
- Bressot C, Aubry A, Pagnoux C, Aguerre-Chariol O, Morgeneyer M. (2018) Assessment of functional nanomaterials in medical applications: can time mend public and occupational health risks related to the products' fate? Journal of Toxicology and Environmental Health, Part A; 1-17.
- Bressot C, Aubry A, Pagnoux C, Aguerre-Chariol O, Morgeneyer M. (2018) Assessment of functional nano-materials in medical applications: Can time mend public and occupational health risks related to the products' fate? *Accepted*. Journal of Toxicology and Environmental Health, Part A: Current Issues.
- Bressot C, Manier N, Pagnoux C, Aguerre-Chariol O, Morgeneyer M. (2017) Environmental release of engineered nanomaterials from commercial tiles under standardized abrasion conditions. Journal of Hazardous Materials; 322: 276-83.
- Bressot C, Shandilya N, Jayabalan T, Fayet G, Voetz M, Meunier L, Le Bihan O., Aguerre-Chariol O, Morgeneyer M. (2018) Exposure assessment of nanomaterials at production sites by a Short Time Sampling (STS) approach strategy and first results of measurement campaigns Process Safety and Environmental Protection; 116: 324-32.
- Cena LG, Peters TM. (2011) Characterization and control of airborne particles emitted during production of epoxy/carbon nanotube nanocomposites. Journal of occupational and environmental hygiene; 8: 86-92.
- Daigle CC, Chalupa DC, Gibb FR, Morrow PE, Oberdorster G, Utell MJ, Frampton MW. (2003) Ultrafine particle deposition in humans during rest and exercise.
- Desotech D. (2006) SOMOS® NanoTool. Book SOMOS® NanoTool, City.
- Ding Y, Kuhlbusch TAJ, Van Tongeren M, Jimenez AS, Tuinman I, Chen R, Alvarez IL, Mikolajczyk U, Nickel C, Meyer J, et al. (2017) Airborne engineered nanomaterials in the workplace-a review of release and worker exposure during nanomaterial production and handling processes. J Hazard Mater; 322: 17-28.

DSM. (2019) Somos PerFORM - A fast processing stereolithography material resulting in strong, stiff and accurate parts with high feature resolution. Book *Somos PerFORM - A fast processing stereolithography material resulting in strong, stiff and accurate parts with high feature resolution*, City.

Göhler D, Nogowski A, Fiala P, Stintz M. (2013) Nanoparticle release from nanocomposites due to mechanical treatment at two stages of the life-cycle. Book *Nanoparticle release from nanocomposites due to mechanical treatment at two stages of the life-cycle*, City: IOP Publishing.

Golanski L, Gaborieau A, Guiot A, Uzu G, Chatenet J, Tardif F. (2011) Characterization of abrasion-induced nanoparticle release from paints into liquids and air. Book *Characterization of abrasion-induced nanoparticle release from paints into liquids and air*, City: IOP Publishing.

Golanski L, Gaborieau A, Guiot A, Uzu G, Chatenet J, Tardif F. (2011) Characterization of machining-induced nanoparticle release from paints into liquids and air. *J Phys: Conf Ser*; 304.

Golanski L, Guiot A, Pras M, Malarde M, Tardif F. (2012) Release-ability of nano fillers from different nanomaterials (toward the acceptability of nanoparticle). *Journal of Nanoparticle Research*; 14: 962.

Gomez V, Levin M, Saber AT, Irusta S, Dal Maso M, Hanoi R, Santamaria J, Jensen KA, Wallin H, Koponen IK. (2014) Comparison of dust release from epoxy and paint nanocomposites and conventional products during sanding and sawing. *Annals of Occupational Hygiene*; 58: 983-94.

Hassan MM, Dylla H, Mohammad LN, Rupnow T. Evaluation of the durability of titanium dioxide photocatalyst coating for concrete pavement," *Construction and Building Materials*, 2010

Hirth S, Cena L, Cox G, Tomović Ž, Peters T, Wohlleben W. (2013) Scenarios and methods that induce protruding or released CNTs after degradation of nanocomposite materials. *Journal of Nanoparticle Research*; 15: 1504.

Huang G, Park JH, Cena LG, Shelton BL, Peters TM. (2012) Evaluation of airborne particle emissions from commercial products containing carbon nanotubes. *Journal of Nanoparticle Research*; 14: 1231.

Jacobs PF. (1992) *Rapid prototyping & manufacturing: fundamentals of stereolithography*: Society of Manufacturing Engineers.

Kahrizangi HS, Sofia D, Barletta D, Poletto M. (2015) Dust generation in vibrated cohesive powders. *CHEMICAL ENGINEERING*; 43: 769-74.

Karim ME, Munir AB, Reza AW, Muhammad-Sukki F, Mohd Yasin SH, Abu-Bakar SH, Abdul Rahim R. (2015) Too enthusiastic to care for safety: Present status and recent developments of nanosafety in ASEAN countries. *Technological Forecasting and Social Change*; 92: 168-81.

Koponen IK, Jensen KA, Schneider T. (2011) Comparison of dust released from sanding conventional and nanoparticle-doped wall and wood coatings. *Journal of exposure science and environmental epidemiology*; 21: 408.

Liguori B, Hansen SF, Baun A, Jensen KA. (2016) Control banding tools for occupational exposure assessment of nanomaterials — Ready for use in a regulatory context? *NanoImpact*; 2: 1-17.

Morgeneyer M, Aguerre-Chariol O, Bressot C. (2018) STEM imaging to characterize nanoparticle emissions and help to design nanosafes paints. *Chemical Engineering Research and Design*; 136: 663-74.

Morgeneyer M, Ramirez A, Smith SM, Tweedie R, Heng J, Maass S, Bressot C. (2018) Particle technology as a uniform discipline? Towards a holistic approach to particles, their creation, characterisation, handling and processing! *Chemical Engineering Research and Design*.

Prototyping M. (2019) *STEREOLITHOGRAPHY*. Book *STEREOLITHOGRAPHY*, City.

Salehi H, Lotrecchiano N, Barletta D, Poletto M. (2017) Dust Release from Aggregative Cohesive Powders Subjected to Vibration. *Industrial & Engineering Chemistry Research*; 56: 12326-36.

Schlagenhauf L, Chu BT, Buha J, Nüesch F, Wang J. (2012) Release of carbon nanotubes from an epoxy-based nanocomposite during an abrasion process. *Environmental Science & Technology*; 46: 7366-72.

Shandilya N, Le Bihan O, Bressot C, Morgeneyer M. (2015) Emission of titanium dioxide nanoparticles from building materials to the environment by wear and weather. *Environ Sci Technol*; 49: 2163-70.

Shandilya N, Le Bihan O, Morgeneyer A. (2014) A Review on the Study of the Generation of (Nano)particles Aerosols during the Mechanical Solicitation of Materials. Journal of Nanomaterials. Sofia D, Giuliano A, Gioiella F, Barletta D, Poletto M. (2018) Modeling of an air quality monitoring network with high space-time resolution. 43: 193-98.

Systems D. (2019) Accura Bluestone (SLA). Book Accura Bluestone (SLA), City.

UE. (2017) DIRECTIVE (EU) 2017/2398 OF THE EUROPEAN PARLIAMENT AND OF THE COUNCIL of 12 December 2017 amending Directive 2004/37/EC on the protection of workers from the risks related to exposure to carcinogens or mutagens at work. <https://eur-lex.europa.eu/legal-content/EN/TXT/HTML/?uri=CELEX:32017L2398&from=FR> In union Tepatcote editor. Book DIRECTIVE (EU) 2017/2398 OF THE EUROPEAN PARLIAMENT AND OF THE COUNCIL of 12 December 2017 amending Directive 2004/37/EC on the protection of workers from the risks related to exposure to carcinogens or mutagens at work. <https://eur-lex.europa.eu/legal-content/EN/TXT/HTML/?uri=CELEX:32017L2398&from=FR> City.

Vorbau M, Hillemann L, Stintz M. (2009) Method for the characterization of the abrasion induced nanoparticle release into air from surface coatings. Journal of Aerosol Science; 40: 209-17.

Wohlleben W, Brill S, Meier MW, Mertler M, Cox G, Hirth S, von Vacano B, Strauss V, Treumann S, Wiench K. (2011) On the lifecycle of nanocomposites: comparing released fragments and their in-vivo hazards from three release mechanisms and four nanocomposites. Small; 7: 2384-95.